Transient growth analysis for axisymmetric pulsatile pipe flows in a rigid straight circular pipe

D. M. Smith and H. M. Blackburn

Department of Mechanical and Aerospace Engineering
Monash University, Clayton, Victoria 3800 Australia

Abstract

We have considered transient growth analysis for a rigid straight circular pipe with a non-zero mean flow rate and single harmonic time-periodic component.

The investigation has been conducted using a spectral element code for varying pulse frequencies and time-periodic amplitudes, bulk flow Reynolds numbers between 500-4000 and azimuthal wavenumbers 0-4.

Variation in the periodic amplitude of the flow was achieved via the ratio of peak flow to bulk flow area averaged flow-rates and was set between 2 and 3. Periodicity was varied according to the reduced velocity - the dimensionless distanced traversed by the bulk flow over one pulse cycle and was either 5 or 10.

The condition producing optimal transient growth of a perturbation was computed on a spectral element mesh scaled for a single axial wavenumber. The peak transient growth was found to scale with Reynolds number squared - a corollary that is also observed in the stability of Hagen-Poiseuille flow (Schmid and Henningson 1994) as well as other parallel shear flows. Changes to the amplitude of the time periodic component only affected the timescale in the evolution of the optimal perturbation.

The largest transient growth was observed for an azimuthal wavenumber of unity and was an order of magnitude larger than for axisymmetric perturbations given similar parameters. Initial optimal perturbations had small axial flow components and were axially invariant for small Reynolds numbers. For an azimuthal wavenumber of unity optimal perturbations appeared as a counter rotating vortex pair in the meridional plane of the pipe.

Introduction

Pulsatile flows in straight, rigid pipes for incompressible Newtonian fluids can serve as idealised models for arterial blood flows as well as for engineering applications for peristalsic flows including microfluidic devices. In either of these cases, understanding the likelihood of turbulent flow as well as how turbulence arises can aid the prevention or promotion of such behaviour.

These flows are driven by the sum of steady and oscillating pressure gradients, and owing to the linearity of the Navier Stokes equations in this case, can be constructed as the superposition of a Hagen Poiseuille flow and oscillatory flow, with the solution to the latter being described by Bessel Fourier functions, first published by (Sexl 1930).

Linear stability analysis for Hagen-Poiseuille flow has found these flows to be asymptotically stable over all Reynolds numbers considered (Schmid and Henningson 1994). Similar studies for oscillatory flows have determined that single harmonic oscillatory flows are also linearly stable over all parameters considered (Yang and Yih 1977). it has been noted that this also implies that any linear combination of steady and oscillatory components is linearly stable ie: pulsatile flows with an arbitrary number of harmonics are linearly stable over all parameters (Nebauer and Blackburn 2009). However, experimental studies have observed turbulence in these flows, and have documented the parameter space over which it is observed (Stettler and Hussain 1986).

Transient stability analysis has been considered for pulsatile flows, however this has been constricted to consider only axisymmetric perturbations (Fedele et. al 2004). The present study aims to extend this work for non-axisymmetric perturbations for single harmonic pulsatile flow.

Base Flows and Problem Parameters

The solution to incompressible flow in a pipe driven by the sum of a steady and oscillating axial pressure gradients K_0 and K_ω respectively was first considered by (Sexl 1930) and later by Womersley (1955). There exists a closed form analytical solution to this problem, shown below in (1) for the axial velocity component.

$$u(r,t) = \frac{R^2 K_\omega e^{i\omega t}}{\mu W_o^2 i} \left[1 - \frac{J_0(i^{\frac{3}{2}} \frac{r}{R} W_o)}{J_0(i^{\frac{3}{2}} W_o)} \right] e^{i\omega t} \tag{1}$$

where pipe geometry is denoted by radius, R and flow properties viscosity, μ and density, ρ. W_o - the Womersley number is a dimensionless frequency parameter defined as $W_o = \sqrt{\rho \omega R^2/\mu}$ where $\omega = 2\pi/T$, T being the pulse period and J_0 is a complex Bessel function. In the case when W_o approaches zero, the period of oscillation grows without bound and the resulting flow-field approaches the standard Hagen-Poiseuille solution and parabolic profiles result.

Given the complexity associated with the Bessel Fourier functions in the base flows it is useful to define an additional term - the instantaneous area-average (bulk) flow rate $\bar{u}(t)$, and represents the flow-rate through a circular cross section of the pipe at particular time. For a pulsatile flow, it is also useful to define the mean flow-rate, $\bar{u}_m$ representing the bulk flow over one pulse cycle.

$$\bar{u}(t) = \frac{8}{D^2} \int_0^{\frac{D}{2}} u(r,t) r dr \qquad \bar{u}_m = \frac{1}{T} \int_o^T \bar{u}_m(t) dt$$

Another term also used to define waveform specific parameters is the peak bulk flow velocity ($\bar{u}_p$) and is defined as the maximum area averaged flow over one pulse cycle.

$$\bar{u}_p = \max \bar{u}(t) \qquad 0 \le t \le T$$

Dimensionless Parameters

There are two dimensionless parameters that can be used to describe the temporal periodicity of the flow - Womersley number and reduced velocity. The Womersley number (W_o) is a dimensionless frequency parameter that can be considered as the ratio

of oscillatory to viscous forces and the reduced velocity (u_{red}) the distance traversed by the bulk flow over one pulse cycle

$$u_{red} = \frac{\bar{u}_m T}{D} \qquad (2)$$
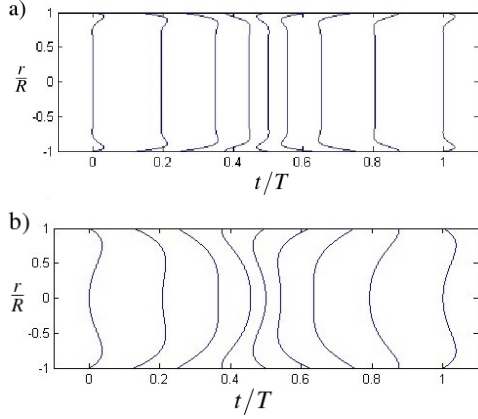
Figure 1: Radial velocity profiles for oscillatory flow a) $w_o = 20$ b) $w_o = 5$.

We only consider pulsatile waveforms with single harmonic, and for this class of base flows it is sufficient to specify a single parameter to describe the waveform - the peak to mean velocity ratio. ($\bar{u}_{pm}$) it is defined as the ratio of peak bulk flow to the mean bulk flow over a single pulse. We consider two waveforms for this study, having peak to mean velocity ratios of two and three in order to investigate the variation associated with flows having stronger oscillatory components. Taking D as the characteristic length scale, and $\bar{u}_m$ as the characteristic velocity scale, the Reynolds number is defined as:

$$\bar{u}_{pm} = \frac{\bar{u}_p}{\bar{u}_m} \qquad Re = \frac{\bar{u}_m D}{\nu} \qquad (3)$$

Radial profiles for oscillatory flow shown in Figure 1 illustrate how these vary between different Womersley numbers for oscillatory flow over a single pulse cycle. At low Womersley numbers, the radial profiles resemble Hagen-Poiseuille flow with almost parabolic profiles at the time of maximum area averaged flow, and at all other times the profiles are flat with sharp gradients near the point of contact with the wall. At high Womersley numbers, the flat profiles are accentuated further, being present at all points during the pulse cycle, while near the walls the velocity profile exhibits distinctive overshoots first noted by Richardson and investigated by Sexl.

Numerical Methods

Transient Stability Analysis

Working in primitive variables and considering flow over a domain Ω the incompressible Navier–Stokes equations can be written as:

$$\partial_t \boldsymbol{u} = -\boldsymbol{u} \cdot \nabla \boldsymbol{u} - \nabla p + Re^{-1} \nabla^2 \boldsymbol{u}, \qquad (\nabla \cdot \boldsymbol{u} = 0), \qquad (4)$$

where p is the kinematic pressure.

The flow-field u can be described as the sum of a steady component, U as well as an arbitrary perturbation to this flow u'. realizing u = U + u' and substituting this into (4) allows for an expression of the time rate of change for the perturbed velocity component.

$$\partial_t \boldsymbol{u}' = -[\boldsymbol{U} \cdot \nabla + (\nabla \boldsymbol{U})^T) \cdot] \boldsymbol{u}' - \nabla p + Re^{-1} \nabla^2 \boldsymbol{u}' \qquad (5)$$

Application of the incompressible flow condition in (4) allows for an expression of pressure in terms of other flow parameters and leads to a partial differential equation of form: $\partial_t \boldsymbol{u}' = \mathcal{L} \boldsymbol{u}'$.

Supposing that a perturbation is an eigenvector of L with eigenvalue greater than or equal to one then this perturbation will grow without bound in time as $\partial_t u' \geq 1$. This can be extended to consider the perturbation at an arbitrary time after the flow has been perturbed through an exponential transformation of (6). This results in finding (complex) eigenvector / eigenvalue pairs of the state transition operator, $A(T)$ in (4) with eigenvalues having magnitudes greater than 1 for a perturbations that will grow in time without bound.

$$A(T) = \exp \int_0^T \mathcal{L} t \, dt \qquad (6)$$

$$\boldsymbol{u}'(T) = A(T) \boldsymbol{u}'(0)$$

If there are no eigenvalues of $A(T)$ with magnitude greater than unity, it is still possible to reach a turbulent state through amplification of a perturbation before it decays. To consider this we examine the ratio of perturbation kinetic energy at time τ normalised by the initial perturbation energy. Defining kinetic energy in the standard way,

$$(u, v) = \int_\Omega u \cdot v \qquad dV \qquad (7)$$

this ratio of energies, $G(\tau)$, is defined using the state transition operator A and its adjoint A^* as

$$G(\tau) = \frac{E(\tau)}{E(0)} = \frac{(A(\tau)u'(0), A(\tau)u'(0))}{(u(0), u(0))} = \frac{(u'(0), A^* A(\tau)u'(0))}{(u(0), u(0)} \qquad (8)$$

Given that the magnitude of $E(0)$ is arbitrary, it can be set to unity, allowing energy growth to be determined entirely by the eigensystem of $A^* A(\tau)$ as the largest eigenvalues correspond to perturbations that experience maximum amplification at τ Letting λ_j and v_j denote an eigenvalue and eigenvenector of $A^* A(\tau)$ respectively, the largest value of $G(\tau)$ that can occur is determined by the eigensystem of $A^* A(\tau)$. Once the eigenvector for maximum amplification has been determined, the flow-field at this time is also known through equation 4, which can be expressed as

$$A(\tau)v_j = \sigma_j u_j. \qquad (9)$$

This corresponds to the singular value decomposition of $A(\tau)$. Therefore, optimum perturbations (v_j), the structure that this develops to at τ are given by the left and right vectors in the singular value decomposition of $A(\tau)$ while the singular values σ_j correspond to the energy amplification of these perturbations at τ. Note that v_i and v_j correspond respectively to pairs of optimal initial and maximum growth perturbations, while $G_j(\tau) = \sigma_j^2$.

Discretization

Discretization in space and time is employed within a cylindrical coordinate spectral element method outlined in Fourier modal structure is assumed in the azimuthal direction of the pipe and the spectral element mesh is employed in a single meridional semi-plane that extends the length of the pipe L_z and from the pipe axis to the outer radius. as shown in Figure 2 below.
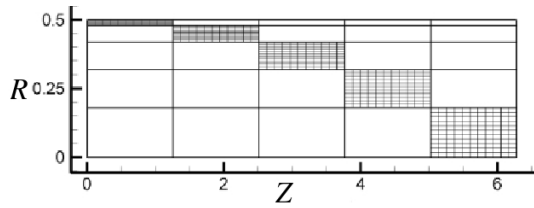
Figure 2: Computational domain used for the transient stability analysis, showing internal nodal points for an axial wavenumber of unity and interpolating polynomial order $N_p = 11$. Note unequal scaling of radial and axial directions.

By assuming Fourier modal structure in the azimuthal direction, it is necessary to consider several azimuthal wavenumbers, but these can be addressed independently owing to linearity of (5). The perturbation is assumed periodic in the axial direction with domain length $L_Z = 2\pi D$. This allows axial wavenumbers $\alpha = 0, 1, ...$ to be included in the analysis for each azimuthal wavenumber.

Transient growth analysis is implemented within a direct numerical simulation (DNS) code outlined by Blackburn and Sherwin (2004) with modifications to include linearized advection operators for both forward and backwards timestepping for application of the joint operator A^*A. This evolution operator is projected onto a Krylov subspace that is of low order so that manipulation of large matrices is not required. From this projection the eigensystem of $A^*A(\tau)$ and hence v_j, u_j and τ_j can be determined These methods are outlined further in Barkley et al (2008)

Results

Transient Growth for m 0-3

Transient growth maxima exhibited a strong dependence on azimuthal wavenumber, with very little growth observed for axisymmetric perturbations and maximum growth observed at an azimuthal wavenumber of unity. Increasing azimuthal wavenumbers above one provided a decline in the transient growth, and this is reflected in figure 3.
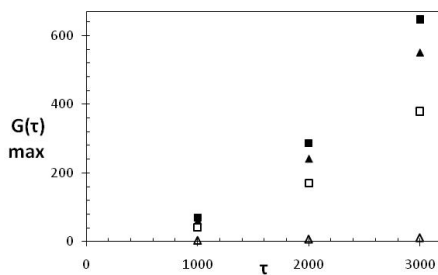
Figure 3: Transient Growth Maxima for $\bar{u}_{pm} = 3$, $m = 0 - 3$ against Reynolds number (empty triangles $m = 0$ empty squares $m = 3$ solid triangles $m = 2$ solid squares $m = 1$)

This may occur because axisymmetric perturbations do not have sufficient freedom to orient themselves in the optimal configuration for maximum transient growth, and this is no longer the case for azimuthal wavenumbers 1 and above. This implies that some azimuthal variation is required for perturbations that are significantly amplified. With larger wavenumbers, too much variation in the azimuthal plane is present, and viscous damping effects severely limit the amplification of these perturbations, and is the reason for diminishing maximum growth for larger wavenumbers.

Although higher azimuthwal wavenumbers exhibit lower transient growth maxima, these maxima are reached over a shorter time, resulting in the tendency for higher azimuthal wavenumbers to be important for the short time transient growth as shown by figure 4. This has also been observed in the transient stability analysis for Hagen-Poiseuille flow by (Schmid and Henningson 1994), for stenotic flow (Blackburn Sherwin and Barkley 2008), and for sudden expansion flows (Cantwell, Barkley and Blackburn 2010). This again suggests that increased azimuthal wavenumber promotes rapid transient growth, but also gives rise to larger viscous forces that cause perturbations to decay over a shorter times.
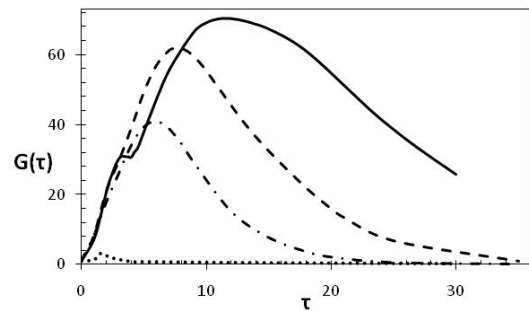
Figure 4: Transient Growth curves for $m = 0 - 3$ at Re 1000, $\bar{u}_{pm} = 3$, $\bar{u}_{red} = 10$ (solid line $m = 1$; dashed line $m = 2$; dotted dash line $m = 3$ dotted line $m = 0$)

Perturbation Structures for Maximum Growth ($m = 1$)

Axial invariance of perturbation structures was observed for the least stable perturbations occurring for azimuthal wavenumber of unity at for low Reynolds numbers, with slight variation developing past a Reynolds number of approximately 1000. The structure within the r-θ plane of the pipe was observed to be a counter rotating vortex pair and is shown below in figure 5. The transient stability analysis for Hagen-Poiseuille flow also identified optimal perturbations for azimuthal wavenumber of unity with little stream-wise dependence (Schmid and Henningson 1994). Additionally, axially invariant modes have been identified as the least stable modes in the asymptotic stability analysis of oscillatory flows (Nebauer and Blackburn 2009).
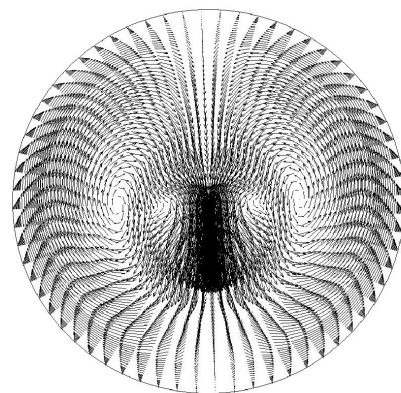
Figure 5: Optimal perturbation structure in the $r - \theta$ plane of the pipe showing counter rotating vortex structure for Re 3500 $m = 1$, $\bar{u}_{red} = 10$ and $\bar{u}_{pm} = 2$

Figure 6 shows how this perturbation has evolved at the point of peak energy by using contours of axial velocity . It is interesting to note that while the initial perturbation was comprised primarily radial and azimuthal flow, it develops to a state where

axial flow provides the majority of the kinetic energy. Also note that this flow is above the threshold for axially invariant perturbations.
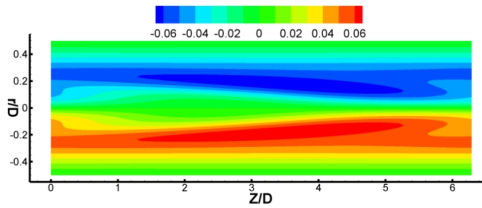
Figure 6: Evolution of the optimal perturbation at the time of maximum growth shown in the meridional semi-plane $\bar{u}_{pm} = 2$, $Re = 3500$ $m = 1$ showing contours of axial velocity (red parallel and blue antiparallel to the pipe axis.

Scaling with Reynolds Number

Maximum transient growth was observed to scale with Reynolds number squared according to $G(\tau)_{max} = 7 \times 10^{-5} Re^2$ and is shown in Figure 7. Kreiss et al (1993) examine bounds for transient energy growth in sub-critical shear flows analytically, and also find a dependence on Reynolds number squared for optimal transient energy growth. While this analysis is restricted to steady flows, it still indicates that parallel shear flows share many of their stability characteristics.
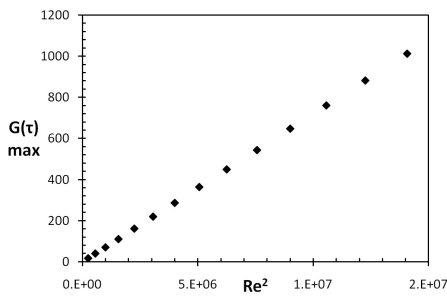
Figure 7: Transient growth curve maxima plotted against the square of Reynolds number ($k = 1$, $\bar{u}_{pm} = 2$)

Variation with $\bar{u}_{red}$ and Waveform

Transient growth maxima do not appear to be sensitive by changes in reduced velocity from 5 to 10 or changes to waveforms with $\bar{u}_{pm}$ varying from 2 to 3. Variation in $\bar{u}_{pm}$ did appear to change the timescale for the evolution of these perturbations by an integer factor of 2, and this is shown below in figure 8. A change in the periodicity appears to have only changed the timescale of the transient growth curves, and might suggest that another dimensionless parameter may suggest some form of coupling between the chosen set of dimensionless parameters as similar effects have been observed in (Nebauer and Blackburn 2009) for the asymptotic stability of oscillatory flows.

Discussion and Conclusions

We have considered the transient stability analysis for pulsatile flows in a rigid straight pipe, and found that transient growth maxima occur for an azimuthal wavenumber of unity and that this growth scales with Reynolds number squared, and were often several orders of magnitude greater than those considered by Fedele et al (2004). Transient growth curves also show that over short times higher azimuthal wavenumbers produce
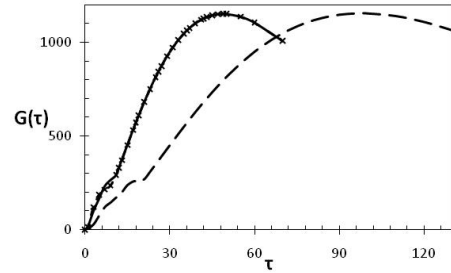
Figure 8: Transient growth envelopes for variations in waveform and periodicity at Re 4000, $m = 1$ $\alpha = 1$. Solid curve: $\bar{u}_{red} = 5$ $\bar{u}_{pm} = 2$; dashed curve; $\bar{u}_{red} = 10$ $\bar{u}_{pm} = 3$ dashed curve with x markers: $\bar{u}_{red} = 10$ $\bar{u}_{pm} = 2$ (curves coincident).

larger growth values, and decay more rapidly. Transient growth dependence scaling with Reynolds number squared has been observed in computational studies (Schmid and Henningson 1994)and also found in analytical studies (Kreiss et al 1993) for other parallel shear flows.

Varying either the reduced velocity or waveform has little effect on the maximum transient growth observed for $m = 1$, and changes to the periodicity of these flows appear to modify only the timescale for the evolution of the transient growth curves, and might suggest some form of coupling between the dimensionless parameters used for this study. Optimum perturbations occurred for an azimuthal wavenumber of unity and were observed as counter rotating vortex pairs in the $r - \theta$ plane of the pipe and little stream-wise variance.

References

BARKLEY, D. BLACKBURN, H. M. SHERWIN, S. J. Direct optimal growth analysis for timesteppers *International Journal for Numerical Methods in Fluids* **57** 1435-1458

BLACKBURN, H. M. SHERWIN, S.J. (2004), Formulation of a Galerkin spectral element-Fourier method for three-dimensional incompressible flows in cylindrical geometries *J. Comput. Phys* **197** 759-778

BLACKBURN, H. M. SHERWIN, S. J. BARKLEY (2008) Convective instability and transient growth in steady and pulsatile stenotic flows. *J. Fluid Mech,* **607** 267 - 277

CANTWELL, C. D. BARKLEY, D. BLACKBURN, H. M. (2010) Transient growth analysis of flow through a sudden expansion in a circular pipe. *Physics of Fluids* **22**

FEDELE, F. HITT, D.L. PRABHU, R.D. (2004) Revisiting the stability of pulsatile pipe flow. *J. Mechanics B/Fluids* , **24** 237-254

NEBAUER, J. BLACKBURN, H. Stability of oscillatory and pulsatile pipe flow 7th *International Conference on CFD in the Minerals and Process Industries*

SCHMID, P. HENNINGSON, D.S. (1994) Optimal energy density growth in Hagen-Poiseuille Flow. *J. Fluid Mech* ,**277** 197-225.

STETTLER, J.C. HUSSAIN A.K.M. On Transition of the pulsatile pipe flow *J. Fluid Mech,* **170** 169-197

SEXL, T. (1930), "Uber den von E. G. Richardson entdeckten 'annulareffekt'" , Z. Phys **61** 179-221

KREISS, G. LUNDBLADH, A. HENNINGSON, S. (1993) Bounds for threshold amplitudes in subcritical shear flows *J. Fluid Mech* **270** 175-198

YANG, W.H. YIH, C.S (1977) Stability of time-periodic flows in a circular pipe, *J. Fluid Mech,* **170** 497-505